



Reverse Separation of Carbon Dioxide and Acetylene in Two Isostructural Copper Pyridine-Carboxylate Frameworks

Jing-Hong Li⁺, You-Wei Gan⁺, Jun-Xian Chen, Rui-Biao Lin,^{*} Yisi Yang, Hui Wu, Wei Zhou, Banglin Chen,^{*} and Xiao-Ming Chen

Dedicated to the 100th anniversary of Sun Yat-Sen University

Abstract: Separating acetylene from carbon dioxide is important but highly challenging due to their similar molecular shapes and physical properties. Adsorptive separation of carbon dioxide from acetylene can directly produce pure acetylene but is hardly realized because of relatively polarizable acetylene binds more strongly. Here, we reverse the CO₂ and C₂H₂ separation by adjusting the pore structures in two isorecticular ultramicroporous metal–organic frameworks (MOFs). Under ambient conditions, copper isonicotinate (**Cu(ina)**₂), with relatively large pore channels shows C₂H₂-selective adsorption with a C₂H₂/CO₂ selectivity of 3.4, whereas its smaller-pore analogue, copper quinoline-5-carboxylate (**Cu(Qc)**₂) shows an inverse CO₂/C₂H₂ selectivity of 5.6. **Cu(Qc)**₂ shows compact pore space that well matches the optimal orientation of CO₂ but is not compatible for C₂H₂. Neutron powder diffraction experiments confirmed that CO₂ molecules adopt preferential orientation along the pore channels during adsorption binding, whereas C₂H₂ molecules bind in an opposite fashion with distorted configurations due to their opposite quadrupole moments. Dynamic breakthrough experiments have validated the separation performance of **Cu(Qc)**₂ for CO₂/C₂H₂ separation.

Introduction

Acetylene is one of important gaseous chemicals in industry,^[1] which can be obtained from gas mixtures coexisting with carbon dioxide after partial combustion of methane or from catalytic cracking of hydrocarbons.^[2] This gas is unstable but important raw material for production of various chemicals such as acrylic acid, vinyl compounds, and 1,4-butanediol. The acetylene molecule shows same linear shape as carbon dioxide molecule with minor difference in their molecular dimensions (C₂H₂: 3.3×3.3×5.7 Å³, CO₂: 3.2×3.3×5.4 Å³). C₂H₂ and CO₂ also have similar boiling points (C₂H₂: 189 K, CO₂: 195 K). And C₂H₂ can be explosive when its gas pressure is above 2 bar. It is therefore very challenging to separate C₂H₂ and CO₂ via approaches based on differentiating their molecular sizes or cryogenic distillation. Therefore, it is of great significance to develop efficient methods for separating C₂H₂ and CO₂ under mild conditions. The approach of adsorptive separation using porous materials is gaining intensive attentions owing to its environmentally friendliness and high energy efficiency.^[3]

As an important type of porous materials, metal–organic frameworks (MOFs) and/or porous coordination polymers (PCPs) have been widely explored for various gas separation.^[3a,d,4] The pore structure of this type of material can be highly adjustable.^[5] Thus, great research endeavors have been devoted to design MOFs with various adsorption sites for separations of C₂H₂ and CO₂. Given that preferential sorption for both gas molecules, those adsorbents can be either C₂H₂-selective or CO₂-selective. Comparing to CO₂, C₂H₂ exhibits a larger polarizability (C₂H₂: 33.3–39.3×10⁻²⁵ cm³, CO₂: 29.1×10⁻²⁵ cm³) and quadrupole moments (C₂H₂: +20.5×10⁻⁴⁰ Cm², CO₂: -13.4×10⁻⁴⁰ Cm²) that can result in stronger nonelectrostatic interactions (including dispersion and induction interactions) with pore surface of adsorbents. Although many MOFs have been reported to show very similar adsorption uptake and/or binding affinity for both C₂H₂ and CO₂, most of them are C₂H₂-selective adsorbents.^[6] For MOFs incorporated with Lewis acidic sites such as open metal sites, the π-complexation interactions with π-electrons of C₂H₂ endow MOFs with subsequent strong binding affinity for that molecule.^[7] However, the open metal sites in MOFs can also interact with electronegative O atoms of CO₂,^[8] which lead to significant CO₂ sorption with poor adsorption selectivity. For MOFs containing Lewis basic moieties such as uncoordinated oxygen

[*] J.-H. Li,⁺ Y.-W. Gan,⁺ J.-X. Chen, Prof. R.-B. Lin, Prof. X.-M. Chen
MOE Key Laboratory of Bioinorganic and Synthetic Chemistry,
GBRCE for Functional Molecular Engineering, School of Chemistry,
IGCME

Sun Yat-Sen University
Guangzhou 510275, China
E-mail: linruibiao@mail.sysu.edu.cn

Dr. Y. Yang, Prof. B. Chen
Fujian Provincial Key Laboratory of Polymer Materials, College of
Chemistry and Materials Science
Fujian Normal University
Fuzhou 350007, China
E-mail: banglin.chen@fjnu.edu.cn

Dr. H. Wu, Dr. W. Zhou
NIST Center for Neutron Research
National Institute of Standards and Technology
Gaithersburg, MD 20899–6102 (USA)

[†] J.-H.L. and Y.-W.G. contributed equally to this work.

and fluoride sites, the formation of hydrogen-bonding interaction between those sites and C_2H_2 molecules can enhance the C_2H_2 adsorption.^[9] However, those sites are also preferential binding sites in many top-performing MOFs for CO_2 capture, as strong electrostatic interactions can be found between O/F atoms with electropositive C sites of CO_2 .^[10]

There are also adsorbents preferentially adsorb CO_2 over C_2H_2 ,^[9] yet the origin of CO_2 -selective adsorption is rarely illustrated. Notably, CO_2 -selective adsorption is conducive for C_2H_2 purification process, because the removal of impurity gas can straightforwardly produce pure C_2H_2 .^[11] Nevertheless, unlike common size-selective separation for various gas mixtures with remarkable molecular size differences, the identical kinetic diameters of both gas molecules (C_2H_2 : 3.3 Å, CO_2 : 3.3 Å) makes it very challenging to predict adsorption preference of porous materials for C_2H_2 and CO_2 . Also, the design of MOFs with preferential binding sites for selective adsorption of CO_2 over C_2H_2 is a tough task. This is because relatively stronger adsorbent-adsorbate interactions can be found between those adsorption sites and relatively more polarizable C_2H_2 , resulting in significant C_2H_2 sorption. In fact, by virtue of the formation of covalent bonds or coordinative bonds with CO_2 molecule, some MOFs can be CO_2 -selective.^[11c,12] The subsequent regeneration of such adsorbents will be highly energy consuming. There are also a few examples of flexible MOFs reported with adsorption preference of CO_2 over C_2H_2 .^[13] However, the mechanisms of such MOFs are not well established, hindering the design of MOFs for the inverse separation.

Given that CO_2 and C_2H_2 show opposite quadruple moments, for pore surfaces with same polarity or electric field gradient, the two gas molecules bind in opposite configurations using either their molecular ends or middle position. This phenomenon is usually observed in MOFs with pore size larger than molecular dimensions of CO_2 and C_2H_2 , when the pore space is large enough for head-on orientation (the rod-shaped molecular perpendicular to the direction of the channel). In contrast, for MOFs with relatively small pore size, especially those close to the molecular size of CO_2 and C_2H_2 , the head-on binding configuration would be kinetically unfavorable in diffusion. Then, as long as the charge distribution on the pore surface complementary to the side-on orientation of CO_2 rather than that of C_2H_2 , CO_2 -selective adsorption can be readily achieved. The π electrons of aromatic conjugated moieties meet such requirement, which are thus targeted to design adsorbents for separation of CO_2 over C_2H_2 .

Copper isonicotinate (**Cu(ina)₂**) and copper quinoline-5-carboxylate (**Cu(Qc)₂**, also known as **Qc-5-Cu-sql**) are isorecticular MOFs with one-dimensional (1D) pore channels,^[14] featuring less-polarizable aromatic rings, which have been demonstrated to be conducive for hydrocarbon recognition.^[14b] In particular, **Cu(Qc)₂** exhibits a relatively small pore aperture of 3.3 Å that is close to the minimum dimensions of both CO_2 and C_2H_2 . Such compact pore space is applicable to study the impact of pore structure adjustment, that is, controlling pore size and electrostatic

potential, on the adsorbent-adsorbate interactions for potential CO_2/C_2H_2 separation in **Cu(Qc)₂**. Herein, gas adsorption experiments show that **Cu(ina)₂** is C_2H_2 -selective with a C_2H_2/CO_2 selectivity of 3.4. In contrast, CO_2 is selective captured in **Cu(Qc)₂** ($66.6\text{ cm}^3\text{ cm}^{-3}$) with a significant preference over C_2H_2 , giving an inverse CO_2/C_2H_2 selectivity of 5.6 at room temperature. Therefore, **Cu(Qc)₂** can preferentially absorb CO_2 from the CO_2/C_2H_2 mixture and produce pure C_2H_2 under ambient condition.

Results and Discussion

Both structures of **Cu(Qc)₂** and **Cu(ina)₂** are composed of 2D coordination networks stacking through π - π stacking interactions, in which each Cu(II) atom is coordinated by two carboxylate groups and two pyridyl/quinoline groups. In their layered structures, Cu(II) atoms serve as 4-connected nodes linked by 2-connected ligands, resulting in square lattice (**sql**) networks (Figures 1 and S1). After the removal of solvent molecules, both **Cu(Qc)₂** and **Cu(ina)₂** show 1D pore channels with accessible void space of 17.2 % and 22.3 %. The sizes of their pore cavities are about $4.7\times 6.1\times 6.6$ and $5.4\times 5.8\times 6.3\text{ Å}^3$, respectively, which can accommodate both CO_2 and C_2H_2 . In particular, their pore apertures at the interconnections of pore cavities are only about 3.3 and 4.1 Å, which match with the size of minimum cross-sectional areas of CO_2 and C_2H_2 molecules (3.3 Å, Table S1). Such size match promotes us to investigate potential effect of pore size on sorption for both gases in these two isorecticular MOFs.

Both **Cu(Qc)₂** and **Cu(ina)₂** were prepared by solvothermal reactions.^[14-15] The PXRD patterns of both as-synthesized samples are consistent with corresponding simulated ones from single crystal data, indicating their bulk products were pure phase. The thermogravimetric analysis (TGA) indicated that **Cu(Qc)₂** and **Cu(ina)₂** can be completely desolvated (Figures S2-4), facilitating to examine their permanent porosities.

Cu(Qc)₂ and **Cu(ina)₂** show similar uptake capacities for CO_2 at 195 K (57 and $65\text{ cm}^3\text{ g}^{-1}$, respectively, see Figure 2a). The Brunauer-Emmett-Teller (BET) surface area of activated **Cu(Qc)₂** and **Cu(ina)₂** was measured to be 238 and $230\text{ m}^2\text{ g}^{-1}$, respectively, (Figure S5). The corresponding experimental pore volume is 0.10 and $0.12\text{ cm}^3\text{ g}^{-1}$, that is basically consistent with their theoretical values from the crystal structures (0.12 and $0.15\text{ cm}^3\text{ g}^{-1}$). The gas adsorption isotherms of **Cu(Qc)₂** and **Cu(ina)₂** for C_2H_2 and CO_2 were then collected at 298 K and sub-atmospheric pressure (Figures 2b and 2d). As expected, **Cu(ina)₂** shows C_2H_2 -selective sorption over CO_2 . For **Cu(ina)₂** at 298 K and 1 bar, its C_2H_2 uptake capacity is $73.8\text{ cm}^3\text{ cm}^{-3}$ (2.18 mmol g^{-1}), and CO_2 uptake capacity is $58.3\text{ cm}^3\text{ cm}^{-3}$ (1.72 mmol g^{-1}), showing a C_2H_2/CO_2 uptake ratio of 127 %. In contrast, **Cu(Qc)₂** exhibits a CO_2 -selective sorption under same condition, with CO_2 uptake capacity of $66.6\text{ cm}^3\text{ cm}^{-3}$ (1.99 mmol g^{-1}) at 1 bar and 298 K, whereas its C_2H_2 uptake capacity is only $26.5\text{ cm}^3\text{ cm}^{-3}$ (0.79 mmol g^{-1}). The CO_2 adsorption capacity of **Cu(Qc)₂** is higher than that of

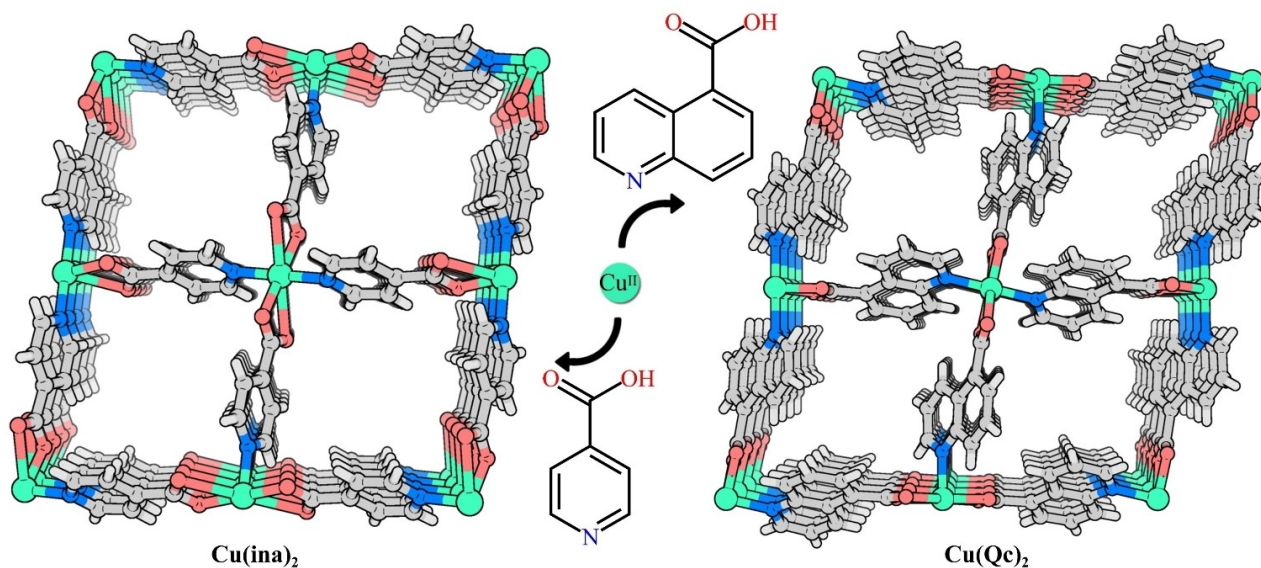


Figure 1. Crystal structures of **Cu(ina)₂** (left) and **Cu(Qc)₂** (right) viewed along the *c*-axis. Cu, C, N, O are represented by light green, gray, light blue, and rose, respectively.

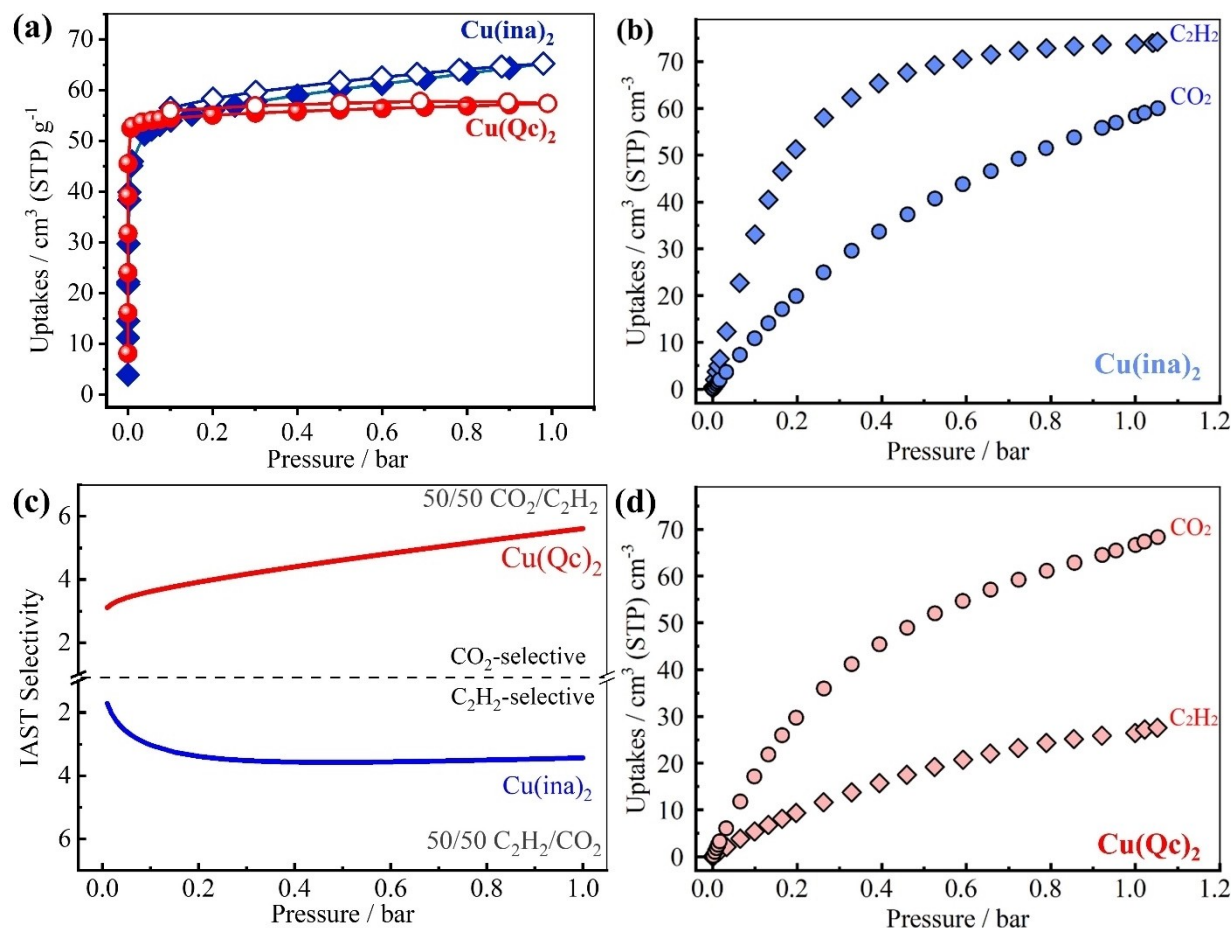


Figure 2. (a) CO₂ sorption isotherms of **Cu(Qc)₂** and **Cu(ina)₂** at 195 K. (b) CO₂ and C₂H₂ sorption isotherms of **Cu(ina)₂** at 298 K. (c) Adsorption selectivities of **Cu(Qc)₂** and **Cu(ina)₂** for equimolar gas mixtures at 298 K and 1 bar. (d) CO₂ and C₂H₂ sorption isotherms of **Cu(Qc)₂** at 298 K.

Cu(ina)₂, that is presumably attributed to the stronger host–guest interactions in **Cu(Qc)₂**. The adsorption amount of C₂H₂ in **Cu(Qc)₂** is significantly lower than that for CO₂, resulting in an uptake ratio of 252 %, higher than those of most other CO₂-selective MOFs whereas lower than that of [Mn(bdc)(dpe)] (640 %, Table S3).^[13b] Notably, according to the amount of adsorbed CO₂ in **Cu(Qc)₂** and the corresponding pore volume, the density of encapsulated CO₂ in the pore channels at 298 K is up to 761 g/liter, which is about 427 times as gaseous CO₂ density of 1.78 g/liter (298 K, 1 bar) and about 65% of the liquid CO₂ density (1178 g/liter at 216.6 K, 5.18 bar), implying the highly efficient packing of carbon dioxide molecules in **Cu(Qc)₂**. In fact, the introduction of large organic substituted groups into host framework can reduce the pore volume, resulting in a decrease of gas uptake capacity in the absence of strong adsorption sites. Indeed, the larger quinoline moieties in **Cu(Qc)₂** dramatically lowered its uptake capacity for C₂H₂. Surprisingly, they showed negligible effect on that of CO₂, as indicated by cycling sorption measurements (Figures S6–7). Obviously, the only thing can be foreseen is that there are different binding configurations between both gas molecules and the framework of **Cu(Qc)₂**. Based on single-component adsorption isotherms of CO₂ and C₂H₂, ideal adsorbed solution selectivity (IAST) theory was then utilized to evaluate the adsorption selectivity of both MOFs (Figures 2c and S8–9). The CO₂-selective **Cu(Qc)₂** shows a selectivity of 5.6 for separation of equimolar CO₂/C₂H₂ mixture at 1 bar and 298 K, which is comparable to those of CO₂-selective MOFs (5–8), such as CD-MOF-1 (5.7),^[12] SIFSIX-3-Ni (7.5),^[11a] PCP-NH₂-ipa (6.4).^[16] In contrast, **Cu(ina)₂** shows an inverse selectivity of 3.4 for separation of equimolar C₂H₂/CO₂ mixture at 1 bar and 298 K. The opposite selectivity and uptake ratio of both MOFs suggested there are different binding affinity for CO₂ and C₂H₂. Coverage-dependent adsorption enthalpies (Q_{st}) of **Cu(Qc)₂** for CO₂ was evaluated from single-component isotherms collected at 273, 298, and 313 K, by using the Clausius–Clapeyron equation (Figures S10–11). The Q_{st} for CO₂ is 31.7 ± 3.5 kJ mol⁻¹ at near zero coverage, which keeps almost constant at higher coverage (Figure S11). Notably, the Q_{st} value for CO₂ is lower than those of typical inorganic porous adsorbents and other CO₂-selective MOFs (Figure S12, Table S2), such as zeolite 4A (33.5 kJ mol⁻¹),^[17] SIFSIX-3-Ni (50.9 kJ mol⁻¹),^[11a] Ionic crystal (38 kJ mol⁻¹),^[13a] [Tm₂(OH-bdc)₂(μ₃-OH)₂(H₂O)₂] (45.2 kJ mol⁻¹),^[18] CD-MOF-1 (41.0 kJ mol⁻¹) and CD-MOF-2 (67.2 kJ mol⁻¹),^[12] en-MOF (71.2 kJ mol⁻¹),^[19] Zn-ox-mtz (43.0 kJ mol⁻¹),^[11d] ALF (47.7 kJ mol⁻¹).^[11e,20] In contrast, the Q_{st} of **Cu(Qc)₂** for C₂H₂ is 21.4 ± 3.5 kJ mol⁻¹ at near zero coverage, which is significantly lower than those of many MOFs (25–79 kJ mol⁻¹),^[7c,8b,9d,21] implying the weak binding affinity of C₂H₂ in relatively compact pore space. In addition, the Q_{st} of **Cu(ina)₂** for C₂H₂ and CO₂ are 27.8 and 24.1 kJ mol⁻¹, respectively (Figures S13–14), which is consistent with the variation of their polarizabilities and adsorption uptakes.

We further mapped the electrostatic potential (ESP) of pore surface in pore channels of **Cu(Qc)₂** by density functional theory (DFT) calculations (Figure S15), where neg-

ative potential are found on conjugated quinoline rings that periodically distributed along the pore channels. By taking the pore size into accounts, the ESP of pore surface in **Cu(Qc)₂** is complementary for CO₂ molecules to arrange along the pore channels (side-on orientations) whereas is not quite compatible for C₂H₂ to interact with aromatic rings. To further investigate the adsorption locates of CO₂ and C₂H₂ in **Cu(Qc)₂**, we performed high-resolution neutron powder diffraction (NPD) measurements (see Supporting Information for details). The binding configurations of CO₂ and C₂D₂ molecules were successfully identified in **Cu(Qc)₂** (Table S3, CCDC number:^[22] 2307752 for [**Cu(Qc)₂]**·0.26 C₂D₂ and 2307753 for [**Cu(Qc)₂]**·0.72 CO₂). As expected, the CO₂ molecules located in side-on orientations with their long axes relatively parallel to the direction of pore channels (Figure 3a–b). The CO₂ molecule interacts with adjacent aromatic rings through π^{δ-}...C^{δ+} interactions (3.15(3)–3.84(2) Å), most of which are slightly shorter than the sum of van der Waals radii of two carbon atoms (3.40 Å), indicating there are considerable electrostatic interactions. These weak electrostatic interactions (π^{δ-}...C^{δ+}) are consistent with the relatively low adsorption heat that would be easily to regeneration.^[11c,23] In contrast, the C₂D₂ molecules bind with the aromatic rings with less stable configurations than their ideal binding model (Figure S16). The ideal head-on binding configuration perpendicular to the plane of aromatic ring is considered as a stable configuration for acetylene molecules, enabling the maximization of their electrostatic interaction with aromatic rings.^[13b] In **Cu(Qc)₂**⊃C₂D₂, C₂D₂ molecules are bound to pore surface through C–D...π interactions. However, the orientation of the binding C₂D₂ molecule in **Cu(Qc)₂** deviates significantly from the ideal head-on binding configuration, which is attributed to the distance between two quinoline rings of 6.1–7.2 Å, being shortly than that of 8.9 Å in ideal head-on binding configuration. Thus, the opposite binding configuration of these two molecules in compact pore space of **Cu(Qc)₂** leads to the inverse selective adsorption of CO₂ over C₂H₂.

To further confirm the preferential adsorption of CO₂ over C₂H₂ by **Cu(Qc)₂**, Grand Canonical Monte Carlo (GCMC) simulation was therefore carried out (Figure S17). The calculated CO₂ and C₂H₂ binding configuration is consistent with the experimental result from NPD data (Figure S18–19). The calculated binding energies for CO₂ and C₂H₂ in **Cu(Qc)₂** are 31.6 kJ mol⁻¹ and 29.4 kJ mol⁻¹, respectively. Overall, compact pore aperture and relatively less stable binding configuration hinder the adsorption of polarizable C₂H₂ that is usually quite strong in common MOFs, thus reverse the selective adsorption. By contrast, the C₂H₂ molecules bound in **Cu(ina)₂** with a larger pore size are closer to the ideal configuration (Figure 3c–d), which enables **Cu(ina)₂** to preferentially adsorb C₂H₂ over CO₂.

To demonstrate the practical CO₂/C₂H₂ separation performance of **Cu(Qc)₂**, column breakthrough experiments were performed, in which gas mixtures of CO₂/C₂H₂/He (5/5/90 v/v/v) flowed over a packed column filled with desolvated **Cu(Qc)₂** at a flow rate of 4.5 mL min⁻¹ at 298 K (Figures 4 and S20). As shown in Figure 4, the CO₂ could be complete

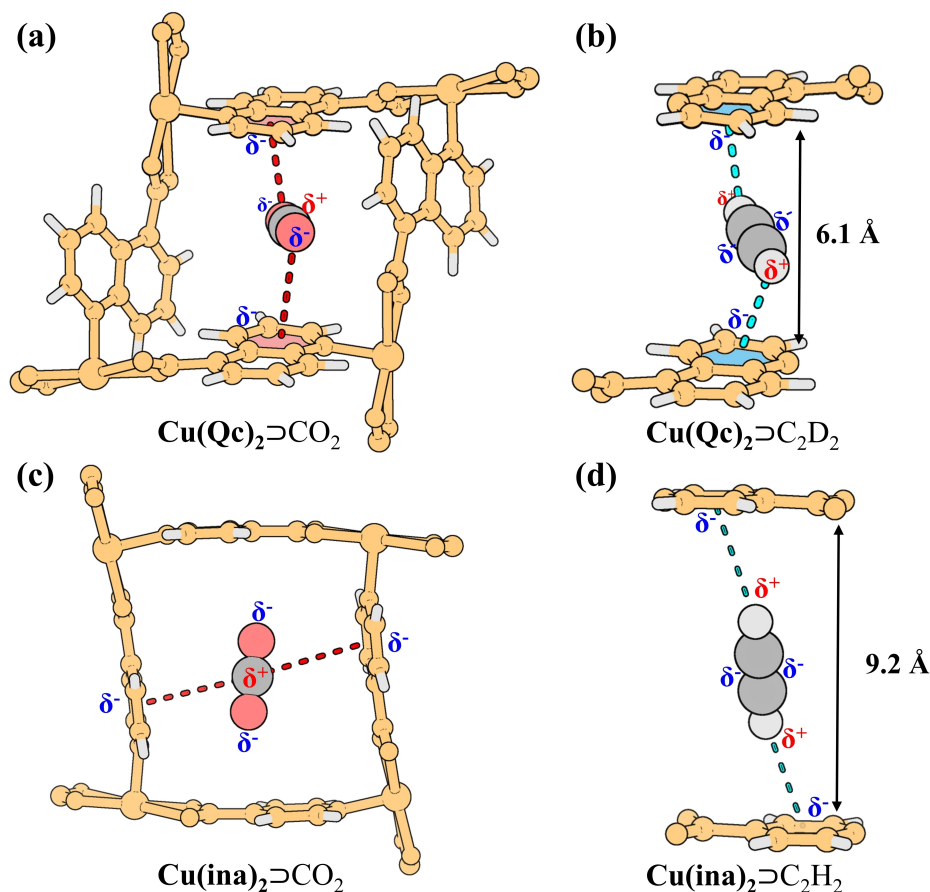


Figure 3. (a) and (b) Neutron diffraction crystal structures of $\text{Cu}(\text{Qc})_2 \cdot 0.72\text{CO}_2$ and $\text{Cu}(\text{Qc})_2 \cdot 0.26\text{C}_2\text{D}_2$ with the close contacts highlighted. (c) and (d) Schematic adsorption sites for CO_2 and C_2H_2 in $\text{Cu}(\text{ina})_2$ obtained from GCMC simulations.

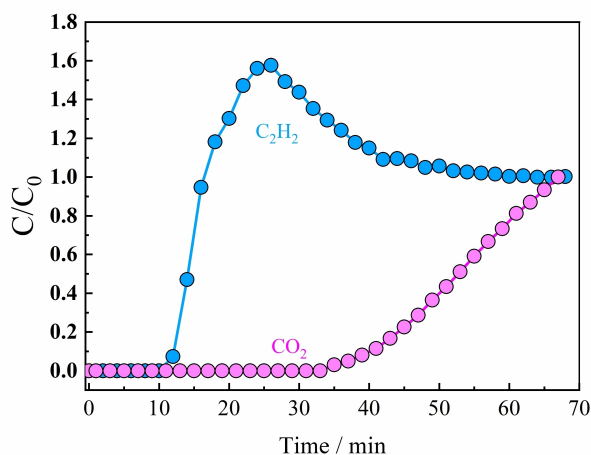


Figure 4. Experimental column breakthrough curves for equimolar $\text{CO}_2/\text{C}_2\text{H}_2$ mixture carried out in a column packed with $\text{Cu}(\text{Qc})_2$ at 298 K and 1 bar.

separation from $\text{CO}_2/\text{C}_2\text{H}_2$ mixture at ambient condition. C_2H_2 was first detected from the outlet and it quickly reached a high purity of 99.9% with no detectable CO_2 . In

contrast, CO_2 was adsorbed in the column during a considerable while until the uptake capacity of $\text{Cu}(\text{Qc})_2$ got saturated. The productivity of high-purity C_2H_2 (>99.9%) was calculated to be 160 mmol per kilogram sorbent, which is comparable with that of CO_2 -selective MOF Cu-F-pymo ($\sim 166 \text{ mmol kg}^{-1}$).^[11b] The practical separation results demonstrated that $\text{Cu}(\text{Qc})_2$ could produce pure C_2H_2 in one single step separation process.

Conclusion

In summary, for MOFs with pore space that is large enough to accommodate optimal binding configurations of C_2H_2 and CO_2 , C_2H_2 -selective adsorption are usually observed because of the relatively more polarizable C_2H_2 . By adjusting the pore size of isoreticular MOFs, we have targeted a CO_2 -selective MOF that can well accommodate CO_2 molecules with optimal orientation but incompatible for that of C_2H_2 molecules. The inverse adsorption of CO_2 over C_2H_2 is thus achieved, leading to relatively straightforward purification of C_2H_2 . This study will inspire future design on microporous MOFs for important separation processes.

Acknowledgements

The authors acknowledge supports from the National Natural Science Foundation of China (22090061, 22375221, 22101307), the Program for Guangdong Introducing Innovative and Entrepreneurial Teams (2017ZT07C069), the Hundred Talents Program of Sun Yat-Sen University.

Conflict of Interest

The authors declare no conflict of interest.

Data Availability Statement

The data that support the findings of this study are available in the supplementary material of this article.

Keywords: ultramicroporous material · gas separation · carbon dioxide · acetylene · reverse

- [1] P. Pässler, W. Hefner, K. Buckl, H. Meinass, A. Meiswinkel, H. J. Wernicke, G. Ebersberg, R. Müller, J. Bässler, H. Behringer, D. Mayer, *Ullmann's Encyclopedia of Industrial Chemistry* **2000**.
- [2] C. E. Webster, R. S. Drago, M. C. Zerner, *J. Am. Chem. Soc.* **1998**, *120*, 5509–5516.
- [3] a) K. Adil, Y. Belmabkhout, R. S. Pillai, A. Cadiau, P. M. Bhatt, A. H. Assen, G. Maurin, M. Eddaoudi, *Chem. Soc. Rev.* **2017**, *46*, 3402–3430; b) R. Banerjee, A. Phan, B. Wang, C. Knobler, H. Furukawa, M. O'Keeffe, O. M. Yaghi, *Science* **2008**, *319*, 939–943; c) H.-G. Hao, Y.-F. Zhao, D.-M. Chen, J.-M. Yu, K. Tan, S. Ma, Y. Chabal, Z.-M. Zhang, J.-M. Dou, Z.-H. Xiao, G. Day, H.-C. Zhou, T.-B. Lu, *Angew. Chem. Int. Ed.* **2018**, *57*, 16067–16071; d) R.-B. Lin, S. Xiang, W. Zhou, B. Chen, *Chem* **2020**, *6*, 337–363; e) E. Pérez-Botella, M. Palomino, S. Valencia, F. Rey, in *Nanoporous Materials for Gas Storage*, Springer **2019**, pp. 173–208; f) S. Yang, A. J. Ramirez-Cuesta, R. Newby, V. Garcia-Sakai, P. Manuel, S. K. Callear, S. I. Campbell, C. C. Tang, M. Schröder, *Nat. Chem.* **2015**, *7*, 121–129; g) L. Yu, X. Han, H. Wang, S. Ullah, Q. Xia, W. Li, J. Li, I. da Silva, P. Manuel, S. Rudić, Y. Cheng, S. Yang, T. Thonhauser, J. Li, *J. Am. Chem. Soc.* **2021**, *143*, 19300–19305; h) H. Zeng, M. Xie, T. Wang, R.-J. Wei, X.-J. Xie, Y. Zhao, W. Lu, D. Li, *Nature* **2021**, *595*, 542–548; i) R.-B. Lin, S. Xiang, W. Zhou, B. Chen, *Chem* **2020**, *6*, 337–363; j) E. J. Kim, R. L. Siegelman, H. Z. H. Jiang, A. C. Forse, J.-H. Lee, J. D. Martell, P. J. Milner, J. M. Falkowski, J. B. Neaton, J. A. Reimer, S. C. Weston, J. R. Long, *Science* **2020**, *369*, 392–396.
- [4] a) R.-B. Lin, L. Li, H.-L. Zhou, H. Wu, C. He, S. Li, R. Krishna, J. Li, W. Zhou, B. Chen, *Nat. Mater.* **2018**, *17*, 1128–1133; b) J. Cui, Z. Zhang, L. Yang, J. Hu, A. Jin, Z. Yang, Y. Zhao, B. Meng, Y. Zhou, J. Wang, Y. Su, J. Wang, X. Cui, H. Xing, *Science* **2024**, *383*, 179–183; c) X.-W. Zhang, C. Wang, Z.-W. Mo, X.-X. Chen, W.-X. Zhang, J.-P. Zhang, *Nat. Mater.* **2023**, *23*, 116–123.
- [5] a) R.-B. Lin, Z. Zhang, B. Chen, *Acc. Chem. Res.* **2021**, *54*, 3362–3376; b) Q.-G. Zhai, X. Bu, X. Zhao, D.-S. Li, P. Feng, *Acc. Chem. Res.* **2017**, *50*, 407–417; c) H. Furukawa, N. Ko, Y. B. Go, N. Aratani, S. B. Choi, E. Choi, A. Ö. Yazaydin, R. Q. Snurr, M. O'Keeffe, J. Kim, O. M. Yaghi, *Science* **2010**, *329*, 424–428.
- [6] a) P. Li, Y. He, Y. Zhao, L. Weng, H. Wang, R. Krishna, H. Wu, W. Zhou, M. O'Keeffe, Y. Han, B. Chen, *Angew. Chem. Int. Ed.* **2015**, *54*, 574–577; b) Y.-P. Li, Y. Wang, Y.-Y. Xue, H.-P. Li, Q.-G. Zhai, S.-N. Li, Y.-C. Jiang, M.-C. Hu, X. Bu, *Angew. Chem. Int. Ed.* **2019**, *58*, 13590–13595; c) K. Shao, H.-M. Wen, C.-C. Liang, X. Xiao, X.-W. Gu, B. Chen, G. Qian, B. Li, *Angew. Chem. Int. Ed.* **2022**, *61*, e202211523; d) X. Wang, H. Liu, Y. Li, X. Yang, F. Gao, X. Wang, Z. Kang, W. Fan, D. Sun, *Coord. Chem. Rev.* **2023**, *482*, 215093; e) Y. Yang, H. Zhang, Z. Yuan, J.-Q. Wang, F. Xiang, L. Chen, F. Wei, S. Xiang, B. Chen, Z. Zhang, *Angew. Chem. Int. Ed.* **2022**, *61*, e202207579; f) J.-P. Zhang, X.-M. Chen, *J. Am. Chem. Soc.* **2009**, *131*, 5516–5521.
- [7] a) S. Uchida, R. Kawamoto, H. Tagami, Y. Nakagawa, N. Mizuno, *J. Am. Chem. Soc.* **2008**, *130*, 12370–12376; b) L. Zhang, K. Jiang, L. Yang, L. Li, E. Hu, L. Yang, K. Shao, H. Xing, Y. Cui, Y. Yang, B. Li, B. Chen, G. Qian, *Angew. Chem. Int. Ed.* **2021**, *60*, 15995–16002; c) Y. L. Peng, T. Pham, P. Li, T. Wang, Y. Chen, K. J. Chen, K. A. Forrest, B. Space, P. Cheng, M. J. Zaworotko, Z. Zhang, *Angew. Chem. Int. Ed.* **2018**, *57*, 10971–10975.
- [8] a) F. Luo, C. Yan, L. Dang, R. Krishna, W. Zhou, H. Wu, X. Dong, Y. Han, T.-L. Hu, M. O'Keeffe, L. Wang, M. Luo, R.-B. Lin, B. Chen, *J. Am. Chem. Soc.* **2016**, *138*, 5678–5684; b) Z. Niu, X. Cui, T. Pham, G. Verma, P. C. Lan, C. Shan, H. Xing, K. A. Forrest, S. Suepaul, B. Space, A. Nafady, A. M. Al-Enizi, S. Ma, *Angew. Chem. Int. Ed.* **2021**, *60*, 5283–5288; c) Y. Wang, X. Jia, H. Yang, Y. Wang, X. Chen, A. N. Hong, J. Li, X. Bu, P. Feng, *Angew. Chem. Int. Ed.* **2020**, *59*, 19027–19030.
- [9] a) X. Cui, K. Chen, H. Xing, Q. Yang, R. Krishna, Z. Bao, H. Wu, W. Zhou, X. Dong, Y. Han, B. Li, Q. Ren, M. J. Zaworotko, B. Chen, *Science* **2016**, *353*, 141–144; b) N. Kumar, S. Mukherjee, N. C. Harvey-Reid, A. A. Bezrukov, K. Tan, V. Martins, M. Vandichel, T. Pham, L. M. van Wyk, K. Oyekan, A. Kumar, K. A. Forrest, K. M. Patil, L. J. Barbour, B. Space, Y. Huang, P. E. Kruger, M. J. Zaworotko, *Chem* **2021**, *7*, 3085–3098; c) R.-B. Lin, L. Li, H. Wu, H. Arman, B. Li, R.-G. Lin, W. Zhou, B. Chen, *J. Am. Chem. Soc.* **2017**, *139*, 8022–8028; d) X. Liu, P. Zhang, H. Xiong, Y. Zhang, K. Wu, J. Liu, R. Krishna, J. Chen, S. Chen, Z. Zeng, S. Deng, J. Wang, *Adv. Mater.* **2023**, *35*, 2210415; e) R. Matsuda, R. Kitaura, S. Kitagawa, Y. Kubota, R. V. Belosludov, T. C. Kobayashi, H. Sakamoto, T. Chiba, M. Takata, Y. Kawazoe, Y. Mita, *Nature* **2005**, *436*, 238–241; f) Y. Ye, S. Xian, H. Cui, K. Tan, L. Gong, B. Liang, T. Pham, H. Pandey, R. Krishna, P. C. Lan, K. A. Forrest, B. Space, T. Thonhauser, J. Li, S. Ma, *J. Am. Chem. Soc.* **2021**, *144*, 1681–1689.
- [10] a) P. Nugent, Y. Belmabkhout, S. D. Burd, A. J. Cairns, R. Luebke, K. Forrest, T. Pham, S. Ma, B. Space, L. Wojtas, M. Eddaoudi, M. J. Zaworotko, *Nature* **2013**, *495*, 80–84; b) S. Ullah, K. Tan, D. Sensharma, N. Kumar, S. Mukherjee, A. A. Bezrukov, J. Li, M. J. Zaworotko, T. Thonhauser, *Angew. Chem. Int. Ed.* **2022**, *61*, e202206613; c) Z. Zhang, S. B. Peh, R. Krishna, C. Kang, K. Chai, Y. Wang, D. Shi, D. Zhao, *Angew. Chem. Int. Ed.* **2021**, *60*, 17198–17204.
- [11] a) K.-J. Chen, H. S. Scott, D. G. Madden, T. Pham, A. Kumar, A. Bajpai, M. Lusi, K. A. Forrest, B. Space, J. J. Perry IV, M. J. Zaworotko, *Chem* **2016**, *1*, 753–765; b) Y. Shi, Y. Xie, H. Cui, Y. Ye, H. Wu, W. Zhou, H. Arman, R.-B. Lin, B. Chen, *Adv. Mater.* **2021**, *33*, 2105880; c) Y. Xie, H. Cui, H. Wu, R.-B. Lin, W. Zhou, B. Chen, *Angew. Chem. Int. Ed.* **2021**, *60*, 9604–9609; d) S.-Q. Yang, R. Krishna, H. Chen, L. Li, L. Zhou, Y.-F. An, F.-Y. Zhang, Q. Zhang, Y.-H. Zhang, W. Li, T.-L. Hu, X.-H. Bu, *J. Am. Chem. Soc.* **2023**, *145*, 13901–13911; e) Z. Zhang, Z. Deng, H. A. Evans, D. Mullangi, C. Kang, S. B. Peh, Y. Wang, C. M. Brown, J. Wang, P. Canepa, A. K. Cheetham, D. Zhao, *J. Am. Chem. Soc.* **2023**, *145*, 11643–11649; f) Y. Li, X.

- Wang, H. Zhang, L. He, J. Huang, W. Wei, Z. Yuan, Z. Xiong, H. Chen, S. Xiang, B. Chen, Z. Zhang, *Angew. Chem. Int. Ed.* **2023**, *62*, e202311419.
- [12] L. Li, J. Wang, Z. Zhang, Q. Yang, Y. Yang, B. Su, Z. Bao, Q. Ren, *ACS Appl. Mater. Interfaces* **2019**, *11*, 2543–2550.
- [13] a) R. Eguchi, S. Uchida, N. Mizuno, *Angew. Chem. Int. Ed.* **2012**, *51*, 1635–1639; b) M. L. Foo, R. Matsuda, Y. Hijikata, R. Krishna, H. Sato, S. Horike, A. Hori, J. Duan, Y. Sato, Y. Kubota, M. Takata, S. Kitagawa, *J. Am. Chem. Soc.* **2016**, *138*, 3022–3030; c) O. T. Qazvini, R. Babarao, S. G. Telfer, *Nat. Commun.* **2021**, *12*, 197; d) N. Yanai, K. Kitayama, Y. Hijikata, H. Sato, R. Matsuda, Y. Kubota, M. Takata, M. Mizuno, T. Uemura, S. Kitagawa, *Nat. Mater.* **2011**, *10*, 787–793; e) Y. Gu, J.-J. Zheng, K.-i. Otake, S. Sakaki, H. Ashitani, Y. Kubota, S. Kawaguchi, M.-S. Yao, P. Wang, Y. Wang, F. Li, S. Kitagawa, *Nat. Commun.* **2023**, *14*, 4245.
- [14] a) K.-J. Chen, D. G. Madden, T. Pham, K. A. Forrest, A. Kumar, Q.-Y. Yang, W. Xue, B. Space, J. J. Perry Iv, J.-P. Zhang, X.-M. Chen, M. J. Zaworotko, *Angew. Chem. Int. Ed.* **2016**, *55*, 10268–10272; b) R.-B. Lin, H. Wu, L. Li, X.-L. Tang, Z. Li, J. Gao, H. Cui, W. Zhou, B. Chen, *J. Am. Chem. Soc.* **2018**, *140*, 12940–12946.
- [15] J. Y. Lu, A. M. Babb, J. Y. Lu, *Chem. Commun.* **2003**, 1346–1347.
- [16] Y. Gu, J.-J. Zheng, K.-i. Otake, M. Shivanna, S. Sakaki, H. Yoshino, M. Ohba, S. Kawaguchi, Y. Wang, F. Li, S. Kitagawa, *Angew. Chem. Int. Ed.* **2021**, *60*, 11688–11694.
- [17] R. J. Harper, G. R. Stifel, R. B. Anderson, *Can. J. Chem.* **1969**, *47*, 4661–4670.
- [18] D. Ma, Z. Li, J. Zhu, Y. Zhou, L. Chen, X. Mai, M. Liufu, Y. Wu, Y. Li, *J. Mater. Chem. A* **2020**, *8*, 11933–11937.
- [19] D. S. Choi, D. W. Kim, D. W. Kang, M. Kang, Y. S. Chae, C. S. Hong, *J. Mater. Chem. A* **2021**, *9*, 21424–21428.
- [20] H. A. Evans, D. Mullangi, Z. Deng, Y. Wang, S. B. Peh, F. Wei, J. Wang, C. M. Brown, D. Zhao, P. Canepa, A. K. Cheetham, *Sci. Adv.* **2022**, *8*, eade1473.
- [21] a) L. Yang, L. Yan, Y. Wang, Z. Liu, J. He, Q. Fu, D. Liu, X. Gu, P. Dai, L. Li, X. Zhao, *Angew. Chem. Int. Ed.* **2021**, *60*, 4570–4574; b) Y. Ye, Z. Ma, R.-B. Lin, R. Krishna, W. Zhou, Q. Lin, Z. Zhang, S. Xiang, B. Chen, *J. Am. Chem. Soc.* **2019**, *141*, 4130–4136.
- [22] Deposition numbers 2307752 (for $[\text{Cu}(\text{Qc})_2] \cdot 0.26 \text{C}_2\text{D}_2$) and 2307753 (for $[\text{Cu}(\text{Qc})_2] \cdot 0.72 \text{CO}_2$) contain the supplementary crystallographic data for this paper. These data are provided free of charge by the joint Cambridge Crystallographic Data Centre and Fachinformationszentrum Karlsruhe Access Structures service.
- [23] C. Yu, Z. Guo, L. Yang, J. Cui, S. Chen, Y. Bo, X. Suo, Q. Gong, S. Zhang, X. Cui, S. He, H. Xing, *Angew. Chem. Int. Ed.* **2023**, *62*, e202218027.

Manuscript received: January 12, 2024

Accepted manuscript online: May 12, 2024

Version of record online: June 17, 2024